Limnol. Oceanogr., 54(2), 2009, 620–629

Downwelling and deep-water bottom currents as food supply mechanisms to the cold-water coral *Lophelia pertusa* (Scleractinia) at the Mingulay Reef complex

Andrew J. Davies[1]
Scottish Association for Marine Science, Dunstaffnage Marine Laboratory, Oban, Argyll, PA37 1QA, UK

Gerard C. A. Duineveld, Marc S. S. Lavaleye, Magda J. N. Bergman, and Hans van Haren
Royal Netherlands Institute for Sea Research, P.O. Box 59, 1790 AB Den Burg, Texel, The Netherlands

J. Murray Roberts
Scottish Association for Marine Science, Dunstaffnage Marine Laboratory, Oban, Argyll, PA37 1QA, UK

Abstract

In 2006 and 2007, multiple deployments of current meters and optical sensors on landers and moorings were made in the first detailed in situ study of the particle supply to the coral community in the Mingulay Reef complex in the Sea of Hebrides at 140-m water depth. Two distinct and predictable supply mechanisms were resolved. One mechanism consisted of the rapid downwelling of surface water caused by hydraulic control of tidal flow that transports particles from the surface to the corals in less than an hour. The rapid downwelling was recorded on the reef top as a pulse of warm, fluorescent, and relatively clear water at the onset of the flood and ebb tides. The pulse was strongest after flood tide and lasted for up to 3 h. The second mechanism consisted of advection onto the reef of deep bottom water with a high suspended matter load. This advection occurred during peak tides and was combined with topographical current acceleration on the reef top, enhancing delivery of particles to the corals.

Cold-water coral communities in the North Atlantic Ocean are dominated by the colonial scleractinian *Lophelia pertusa* (Linnaeus 1758). They have been mainly reported from bathyal depths on the continental shelf and slope and are usually found on sloping topography or local highs such as offshore banks, seamounts, and coral carbonate mounds (Frederiksen et al. 1992; Rogers 1999). In some cases, topography supporting live cold-water corals is the result of growth of the corals giving rise to formation of an extensive reef framework that over glacial–interglacial time periods can develop coral carbonate mounds of several hundreds of meters in height (Roberts et al. 2006; Williams et al. 2006; Kano et al. 2007) that support biodiversity-rich communities (Henry and Roberts 2007; Roberts et al. 2008). Besides extensive cold-water coral communities covering deep-water mounds (~600 m) such as the Porcupine and Rockall banks (van Weering et al. 2003), coral communities have also developed locally on sills and banks in relatively shallow water (100–200 m) off the Scottish and Norwegian coasts (Freiwald et al. 2002; Jonsson et al. 2004; Roberts et al. 2005).

The structure and functioning of deep-water benthic communities living in topographically complex settings (canyons, slopes, seamounts) is thought to be strongly dependent on the interplay between water flow and seafloor relief, as this determines the supply of food particles and larvae (Flach and Thomsen 1998; Gage et al. 2000; Hughes and Gage 2004). In some situations, the interaction between currents, internal waves, and topography creates suitable conditions for the development of rich benthic communities dominated by suspension-feeding cold-water corals (Genin et al. 1986; White et al. 2005, 2007). The preferential occurrence of cold-water corals on seafloor relief has been often explained by the topographic acceleration of near-bed currents that enhances food supply (Mortensen et al. 2001; Thiem et al. 2006; Kiriakoulakis et al. 2007). In some locations, internal waves have been found or assumed to play a role in food supply to cold-water coral communities. Around the Faroe Islands, Frederiksen et al. (1992) reported highest *L. pertusa* abundances in areas where the seabed slope is critical to the ray of an internal wave. They suggested that these regions may have locally intensified currents and that breaking internal waves may ultimately enhance local food availability for cold-water corals. These waves may improve conditions for coral growth by redistributing suspended particles in near-bed mixing layers and may also promote surface productivity by increasing the vertical nutrient flux. Internal waves have also been found to transport fresh phytoplankton to the cold-water corals

[1] Corresponding author (andrew.davies@sams.ac.uk).

Acknowledgments

We thank the crew of the RV *Pelagia* for their dedication and assistance in collecting field data. The manuscript was improved by comments from Martin White, Andrew Dale, and two anonymous reviewers.

This work was supported by the European Hotspot Ecosystem Research on the Margins of European Seas project (contract GOCE-CT-2005-511234) funded under the priority "Sustainable Development, Global Change and Ecosystems" (to G.C.A.D. and J.M.R.) and the Trans-Atlantic Coral Ecosystem Study project (EC contract MOIF-CT-2006-040018) under the program "Structuring the European Research Area" (to J.M.R.), both funded by the European Commission's Sixth Framework Program.

covering the giant coral carbonate mounds in the Southeast Rockall Trough (Duineveld et al. 2007; Mienis et al. 2007).

The diet of cold-water corals forms a critical issue in discussions and inferences about their mechanisms of food supply. Cold-water corals were thought to be sustained by local hydrocarbon seepage and chemoautotrophic production (Hovland and Thomsen 1997). Data obtained so far indicate that cold-water coral communities rely on the delivery of phytoplankton, organic matter, and perhaps zooplankton derived from near-surface primary productivity (Duineveld et al. 2004, 2007; Kiriakoulakis et al. 2005). Lateral and vertical advection of particles may therefore play an important role in the functioning of coral ecosystems. Few studies have conclusively recorded food-supply mechanisms to a cold-water coral reef in situ. Here, we report on in situ measurements of currents, temperature, turbidity, and fluorescence made in a cold-water coral community on a reef in the relatively shallow strait between the Outer Hebridean Island chain and the Scottish mainland. The data were collected over 2 yr (2006–2007) with the aim of finding predictable food-supply mechanisms that could explain the presence of the local cold-water coral community.

Methods

Study area—The Mingulay Reef complex is located to the east of the island of Mingulay in the Sea of Hebrides (Fig. 1, inset). In 2003, areas suspected to contain cold-water corals were mapped by multibeam echosounder and several reefs formed by *L. pertusa* were discovered (Roberts et al. 2005). The largest known area with a cover of living coral is Mingulay Reef 1, which occurs as an extension to a rocky sill. The reef and bank complex is approximately 4 km long and 500 m wide (Fig. 1). Subsequent multibeam mapping of the Mingulay area was conducted in summer 2006 using a Kongsberg-Simrad EM300 multibeam echosounder on board the RV *Pelagia*. The system was a 30-kHz echosounder that used 135 beams per ping over a maximum coverage sector of 150° (beam spacing was equidistant), and was capable of producing detailed bathymetric maps that allowed accurate placement of moorings and benthic landers on the steep and rugged topography of Mingulay Reef 1.

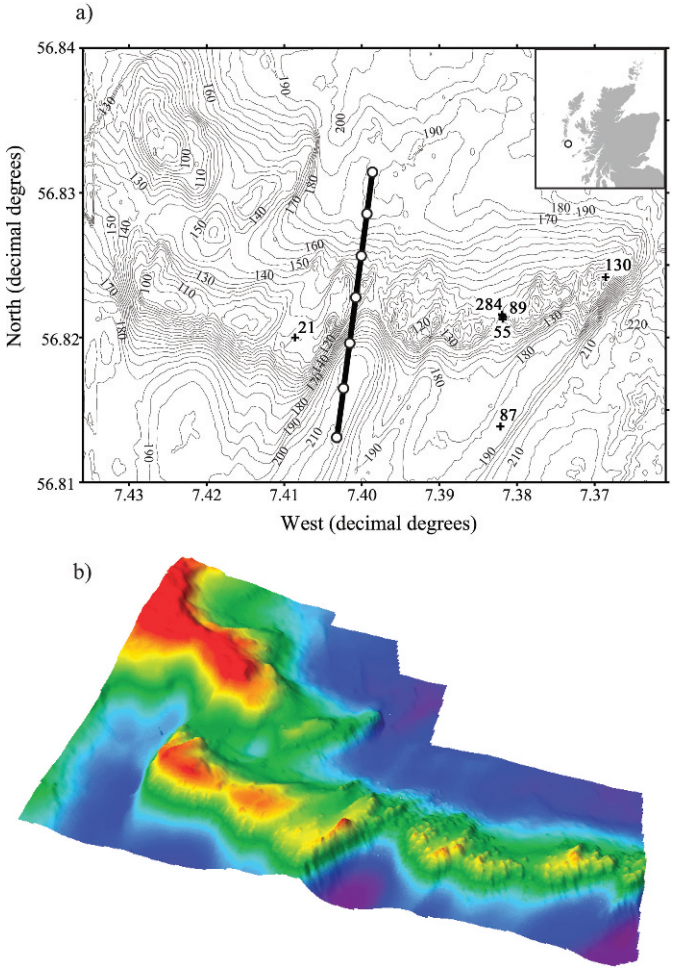

Fig. 1. (a) Bathymetry of the Mingulay Reef 1 generated from multibeam data. The locations of principal mooring and lander deployments in Table 1 are shown. The line shows the direction of the north to south CTD transect in July 2006 across the central and western part of Mingulay Reef 1 with the circles showing individual CTD locations. The inset shows the location of the Mingulay Reef 1 (circle) in relation to the UK landmass (projection used is universal transverse Mercator). (b) Three-dimensional map of Mingulay Reef 1 showing the steep southern face and the sloping northern face.

In situ measurements—A series of moorings and autonomous benthic landers were deployed around Mingulay Reef 1 for various periods (Fig. 1; Table 1). The moorings consisted of an Aanderaa RCM-11 current meter (Aanderaa Data Instruments) and a set of optical back scattering (OBS) and fluorescence sensors (Seapoint) connected to a data logger (Netherlands Institute for Sea Research) that also recorded temperature. The moorings were held upright by 6 Benthos floats, with the current meter and logger positioned 2.5–3.5 m above the seafloor (Table 1). The moorings were supplemented by deployments of the autonomous lander for biological experiments (Duineveld et al. 2004). The lander consisted of an aluminum tripod frame equipped with 12 glass Benthos floats, two acoustic releases, and a single 250-kg ballast weight. The lander carried the following instruments: (1) a FSI three-dimensional (3D) acoustic current meter (Falmouth Scientific), (2) a Seapoint OBS for measuring turbidity, and (3) a Seapoint fluorometer for measuring fluorescent particles in the water column; all lander instruments were mounted at 1 m above bottom, recording horizontally rather than downward. Variables were recorded at 1- or 2-min intervals throughout the duration of each deployment at 2 Hz (two times per second). Calibration of the Seapoint OBS was not conducted because calibrations are material specific and can be unreliable over long deployments because of a variety of different materials encountered. Instead the values presented in the plots are relative (volts) and linearly proportional to suspended solid concentration.

At the end of the cruise in June 2007 a mooring was deployed at the top of Mingulay Reef 1 for a period of 3 months (Sta. 284, Table 1). The instrumentation differed

Table 1. Descriptions of the mooring and lander deployments on Mingulay Reef 1.

Station no.	Height of instruments above seabed (m)	Type	Depth (m)	Deployment date and time	Recovery date and time
21	2.5	Mooring	119	11 Jul 06 17:00 h	13 Jul 06 17:00 h
55	2.5	Mooring	129	14 Jul 06 13:30 h	17 Jul 06 09:30 h
87	2.5	Mooring	188	17 Jul 06 17:00 h	21 Jul 06 16:00 h
89	1	Lander	136	18 Jul 06 07:00 h	19 Jul 06 06:00 h
130	1	Lander	123	20 Jul 06 13:00 h	21 Jul 06 17:00 h
284	2.5	Mooring	129	27 Jun 07 09:00 h	24 Sep 07 09:00 h

slightly from the short-term moorings, consisting of an Aanderaa RCM-9 current meter, a fluorometer, and OBS (Wetlabs) connected to a UMI-2SB7 data logger (W.S. Ocean Systems). The position of the mooring was close (125 m) to Sta. 55 (Fig. 1).

Conductivity, temperature, depth (CTD) profile and yo-yo—On 10 July 2006 a CTD transect was made across the center of Mingulay Reef 1 (Fig. 1). The unit consisted of a SBE 911 CTD (Sea-Bird Electronics) including auxiliary sensors for turbidity (Seapoint) and fluorescence (Aqua III, Chelsea Technologies Group). The transect consisted of a total of seven stations approximately 300 m apart covering a distance of ~2 km. At each station the CTD was lowered and raised from the seafloor before moving to the next station. Measurements started at the northernmost point of the transect at 14:22 h universal time, coordinated (UTC) and ended at its southern point at 16:22 h. This time period falls just after the time that the flood tide turns to ebb.

On 20 June 2007 a yo-yo CTD series was made on the eastern summit of Mingulay Reef 1 while the ship was kept at a position close to that of Sta. 55 (Fig. 1). The configuration of the CTD was similar to that in the 2006 cruise. The yo-yo series consisted of 43 CTD casts covering a tidal cycle from 06:32 h to 19:20 h UTC. The CTD yo-yo coincided with a mooring on Mingulay Reef 1 that was down from 17 to 22 June at the position of Sta. 55. The mooring data showed that on 20 June the ebb–flood and flood–ebb change took place at 05:45 h and 12:00 h UTC, respectively. Vertical profiles of temperature, fluorescence, and turbidity were plotted against time using Surfer (Golden Software).

Cross-correlation function analysis—The synchronicity between the variables measured with the moorings and landers (temperature, fluorescence, and turbidity) was assessed using cross-correlation function (CCF) analysis. CCF measures the correlation between two time series with different time offsets (lag). In the current study, the plots of cross-correlations as a function of a lag interval (represented as hours) were used to compare the effect of current speed on other variables. Positive lags represent the primary axis offset against the secondary axis, whereas negative lags represent the secondary axis offset against the primary axis.

Results

Moorings and landers—The predominant flow direction of the surface water in the channel between the Outer Hebrides and the Scottish mainland has a SSW-NNE orientation (tidal stream atlas, UK Admiralty Office). The reef and bank lie perpendicular to the current in a W-E orientation, and rise 40 to 80 m above the surrounding area (approximately 180–200 m depth, *see* Fig. 1). This structure is therefore expected to form a serious obstruction to the tidal flow and to exert control over the strength and direction of the flow. On top of Mingulay Reef 1 at ~130-m water depth, tidal currents still have a SSW-NNE direction, as shown by mooring data collected on the eastern and western crests of Mingulay Reef 1 (Stas. 21, 55, 89, 130; Fig. 2). However, near the reef base (Sta. 87), currents have more SW-NE directions because of deflection by the reef topography (Figs. 1, 2). Data summarized from all the deployments conducted during the two expeditions in 2006 and 2007 showed that the currents are largely tidal, with their strength altered by the topography. On the easternmost part of the reef at Stas. 55 and 89, mean current amplitude reached 29 cm s^{-1} with a peak of 81 cm s^{-1}. The western part of Reef 1 at Sta. 21 appeared to be somewhat more sheltered from tidal currents, with a mean amplitude of 22 cm s^{-1} and a peak of 67 cm s^{-1}. At the base of the reef (Sta. 87) the mean current amplitude over a tidal cycle was 12 cm s^{-1}, with a maximum of 26 cm s^{-1}.

In every deployment made on Mingulay Reef 1 in 2006 and 2007, a distinct pulse of warm water was observed near the bottom at the onset of the ebb tide. During the change from ebb to flood a similar peak occurred but this was less pronounced and sometimes absent. The pattern is illustrated in Fig. 3a, showing records from a high-resolution 3D mooring deployment at Sta. 55 (Fig. 1). During the pulse the temperature rose by 0.75°C to reach 10.25°C and this persisted for ~3 h maximum. A much smaller increase in temperature of only 0.2°C was recorded during the change from ebb to flood (Fig. 3a). Concurrently with the warm pulse, fluorescence levels doubled. Turbidity levels were on average lower during the warm pulse. This is not very clear in the particular record in Fig. 3a because of high variability in turbidity but appeared statistically significant in other records (*see* section below). The above pattern is highly consistent and was recorded in all 2006 deployments on Mingulay Reef 1 and again in 2007 when a mooring was deployed for 3 months (Sta. 284, Table 1). The 3-month record showed that the pulse of warm and fluorescent water was relatively strongest during spring tide currents (Fig. 3b). This was supported by CCF analysis after the 12-h tidal cycle had been removed by low pass filtering. In the

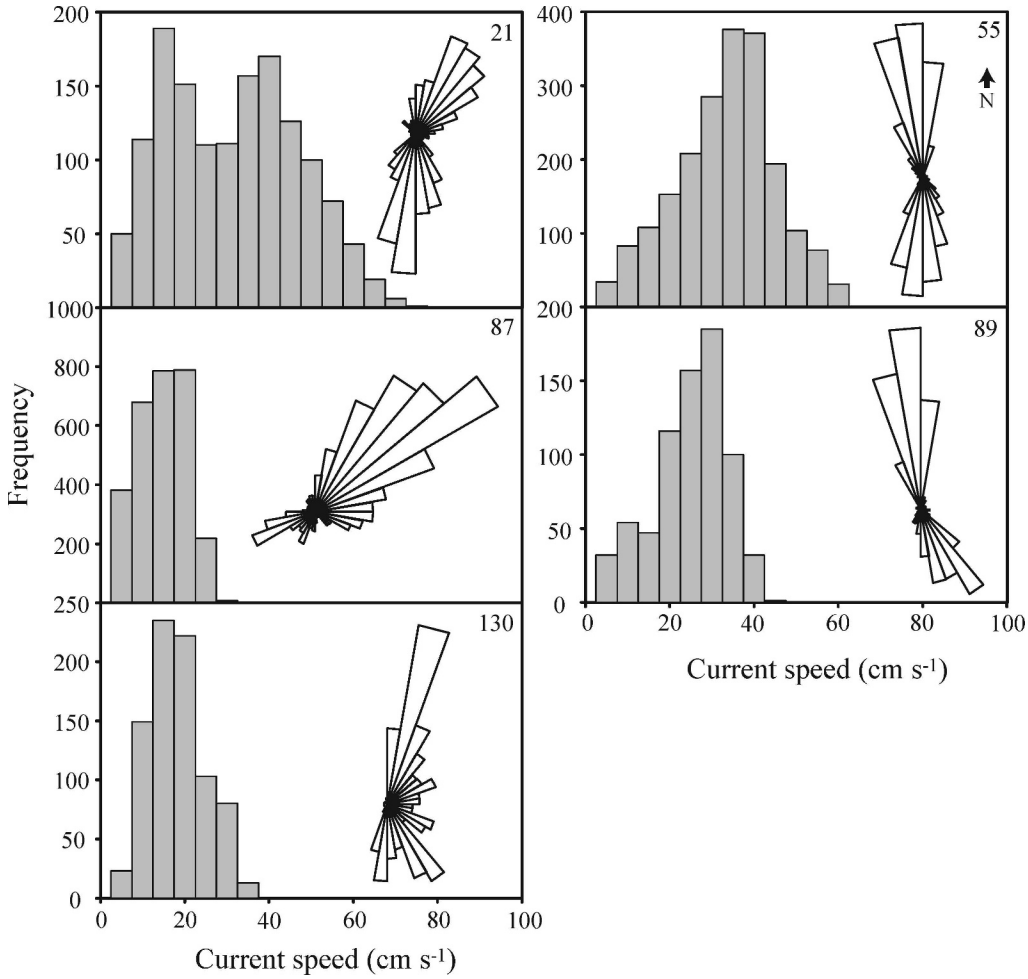

Fig. 2. Frequency distributions of near-bottom current speed and directional histograms on the basis of mooring and lander deployments on top and at the base of Mingulay Reef 1 in July 2006. The arrow in panel Sta. 55 indicates north direction for all stations.

smoothed series containing only variation due to neap and spring cycles, current speed and fluorescence were significantly correlated (Pearson's $r = 0.46$, $p < 0.0001$).

CTD profiles—During the 2006 cruise a CTD transect was made across the central part of Mingulay Reef 1 shortly after the onset of ebb tide to capture the structure of the water column over a wider reef area (2 km). Logistical constraints prevented us recording the onset of ebb when the pulse is strongest. However, the CTD transect was made near spring tide when the pulses are generally stronger, including the small flood pulse. The vertical profiles of temperature, salinity, fluorescence, and turbidity in Fig. 4 show a downward bending and compression of isotherms and isohalines to the north of the summit, indicative of surface water reaching the depths of the reef. This surface water had a higher temperature and fluorescence but lower salinity and turbidity. Isopleths of turbidity suggest that the warmer water displaces water with higher turbidity that probably originates from the reef base and surrounding area.

In 2007 another series of CTD profiles were recorded to capture the water column structure during the warm water pulse. This time, a yo-yo series of CTD casts was made at a single station on the eastern summit of Mingulay Reef 1 near Sta. 55. The profiles of temperature, salinity, and fluorescence (Fig. 5) clearly demonstrate a downward movement of surface water 1 to 2 h after the start of measurements at the onset of the flood tide. A second event was also seen in the temperature, salinity, and sigma theta profiles at the onset of the ebb tide at approximately 13:30 h UTC. Then toward the end of the series, approximately a tidal cycle after the first event, there is a larger event that was similar in strength to the first. The rapid downwelling during the warm pulse was also picked up by a 3D current meter of a mooring that had been previously deployed at Sta. 89 on the eastern Reef 1 area (Fig. 6). That record shows a near-perfect inverse relationship between the rapid downwelling represented by the vertical water movement and temperature during the first downwelling event. The largest downwelling event occurs during the transition from northward to southward flow, which is from the flood to ebb tide, with a smaller event occurring during the ebb to flood tide (Fig. 3a).

Correlations between variables—Cross-correlations between tidal patterns in current speed and other variables

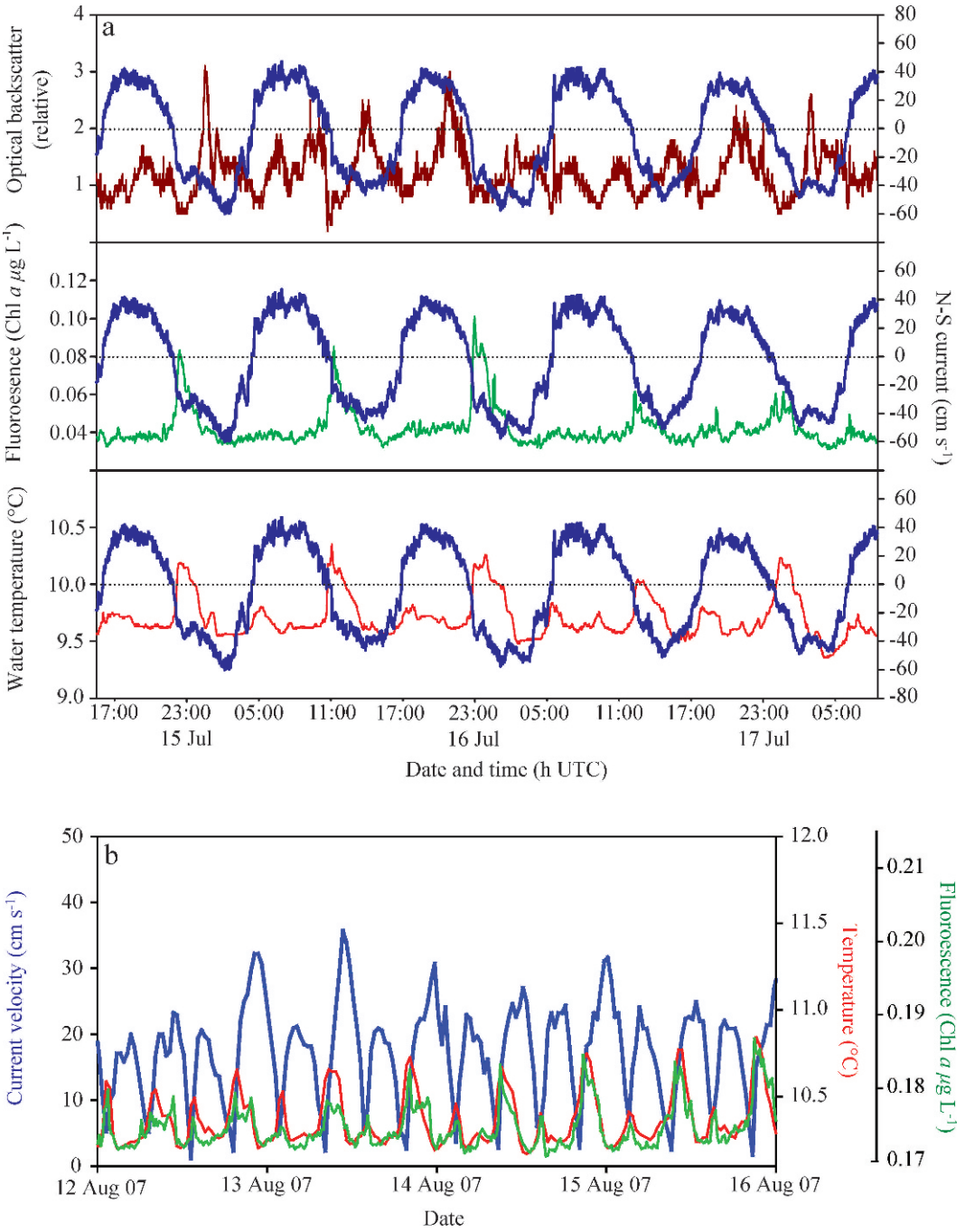

Fig. 3. (a) Relationship between the current speed in N-S direction (blue line) and turbidity (top, brown line in relative units, *see* text), fluorescence (middle, green line), and temperature (bottom, red line). Recordings were made on the summit of Mingulay Reef 1 (Sta. 55) and data represent 10-min moving averages. (b) Excerpt of a 3-month record of current speed, fluorescence, and temperature measured in 2007 at Sta. 284. Note the 2007 mooring had a different set of instruments (*see* text).

yielded significant coefficients with and without primary time lags of plus or minus an hour (Fig. 7). The strong and symmetric periodicity in the cross-correlations implies that these processes are regular throughout the time series, with the most significant delivery of surficial water occurring on a M2 semidiurnal cycle (Fig. 7). Current speed and turbidity were significantly positively correlated with a time lag +1 h (Fig. 7b), which means that turbidity increases 1 h after the increase of the current speed. The cross-correlation between the records of near-bottom current speed and fluorescence yielded a positive correlation with a time lag of −1 h (Fig. 7c). This suggests that the warm fluorescent pulse followed slack water and current speed did not affect the concentration of fluorescent particles on the reef by resuspension. Temperature is significantly correlated without a time lag with turbidity (negative) and with fluorescence (positive) (Fig. 7d,e). This illustrates the intrinsic linkage of these variables in the form

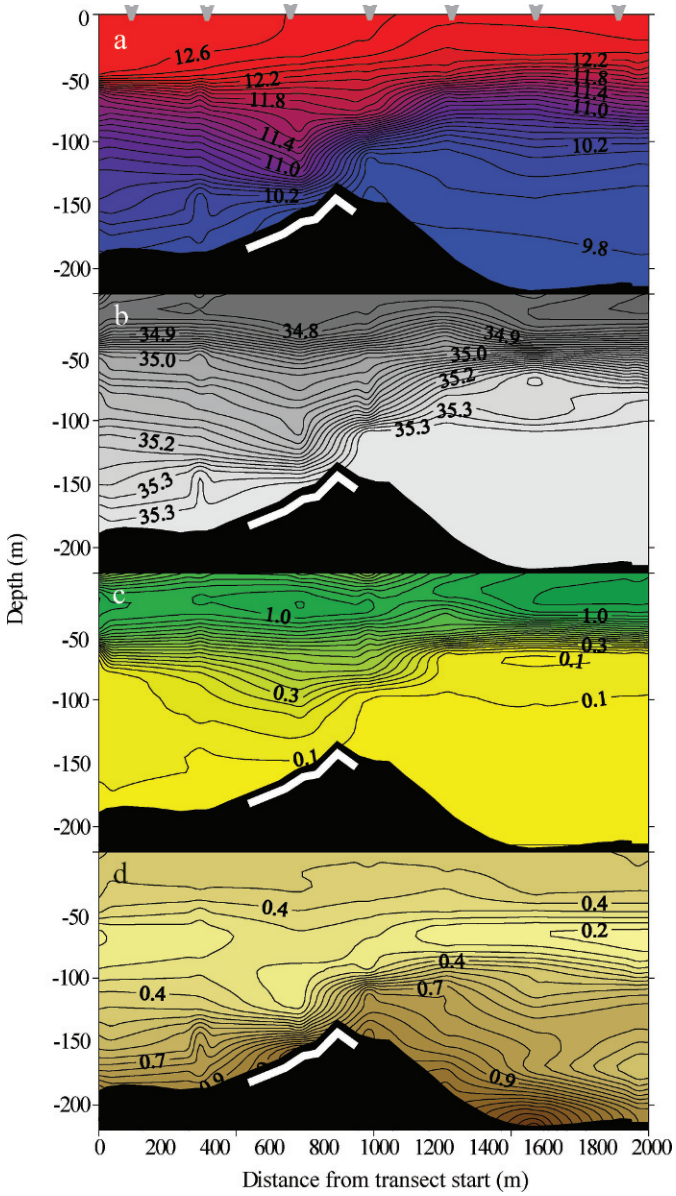

Fig. 4. CTD transect across the center of Mingulay Reef 1 (for position *see* Fig. 1). The white bar represents areas of dense coral framework; gray arrows in the upper panel are individual CTD locations. The values along the *x*-axis represent the distance from the start at the north end of the transect. Recorded variables from top to bottom: (a) temperature (°C), (b) salinity, (c) fluorescence (Chl *a*, μg L^{-1}), and (d) turbidity (formazin turbidity standard, FTU). The profiles represent the situation after the onset of ebb tide.

of a pulse of warm, fluorescent, and relatively clear surface water (Fig. 3a).

Discussion

The mechanisms that supply food to cold-water coral communities and the nature of the food itself has, to date, been inferred from two sources: general hydrographic processes occurring where corals are found and from nutritional biomarker analysis of coral samples. The consensus is that accelerated currents associated with topographic relief enhance particle supply to cold-water corals (Thiem et al. 2006). This assumes that cold-water corals primarily feed on particles in the benthic boundary layer that are resuspended (by turbulent friction) and advected by (tidal) currents. Depending on their residence time near the bottom, such particles may have low nutritional content because of the high microbial activity in the benthic boundary layer (Ritzrau et al. 1997). Here, in situ observations show that the food supply that sustains *L. pertusa* reefs originates from outside of the reef area, driven by a complex interplay between topography and tides. The rapid downwelling event can have a velocity up to 10 cm s^{-1}. In the 19-h selection of the measurements of the near-bottom current shown in Fig. 6 the vertical downward velocity exceeds 5 cm s^{-1}. Therefore, particles from the surface can be transported to the corals at 140-m depth in less than 1 h. The fluorescent matter supplied by the rapid downwelling is probably a utilizable energy source for *L. pertusa*. Isotope signatures (δ^{15}N) of *L. pertusa* on a coral carbonate mound off Ireland showed that the corals have the same trophic level, and possibly also food source, as bivalves and tunicates, which are obligate filter-feeders living on small organic particles including algae (Duineveld et al. 2007).

Several possible physical explanations are available that can describe the rapid downwelling observed at Mingulay, and also for other mechanisms of turbulent transport that occur at shallow banks. The most likely are the hydraulic control of flow over topography, or the trapping and breaking of nonlinear internal waves, which also can transport matter to shoaling topography (Valle-Levinson and Wilson 1994; Farmer and Armi 1999). Internal hydraulic jumps have been associated with modified density and flow structure near small banks (Nash and Moum 2001). In a tidal situation, hydraulic control of the flow over a bank can lead to a depression of the density structure downstream of it. When the tidal flow weakens and reverses, this depression propagates as an internal wave over the summit in the previously upstream direction.

To determine whether the tidal flow over the Mingulay Reef 1 could be hydraulically controlled, an internal Froude number (*Fr*) was calculated,

$$Fr = \frac{u}{c} \tag{1}$$

In a hydraulically controlled situation, the flow speed u matches the internal wave phase speed, so $Fr = 1$. Here, c is estimated as:

$$c = \frac{NH}{\pi} \tag{2}$$

by assuming uniform stratification, where N is the buoyancy frequency from the CTD profile:

$$N^2 = \frac{g}{\rho}\frac{\Delta\rho}{H} \tag{3}$$

g is the gravitational constant, ρ is the typical density for

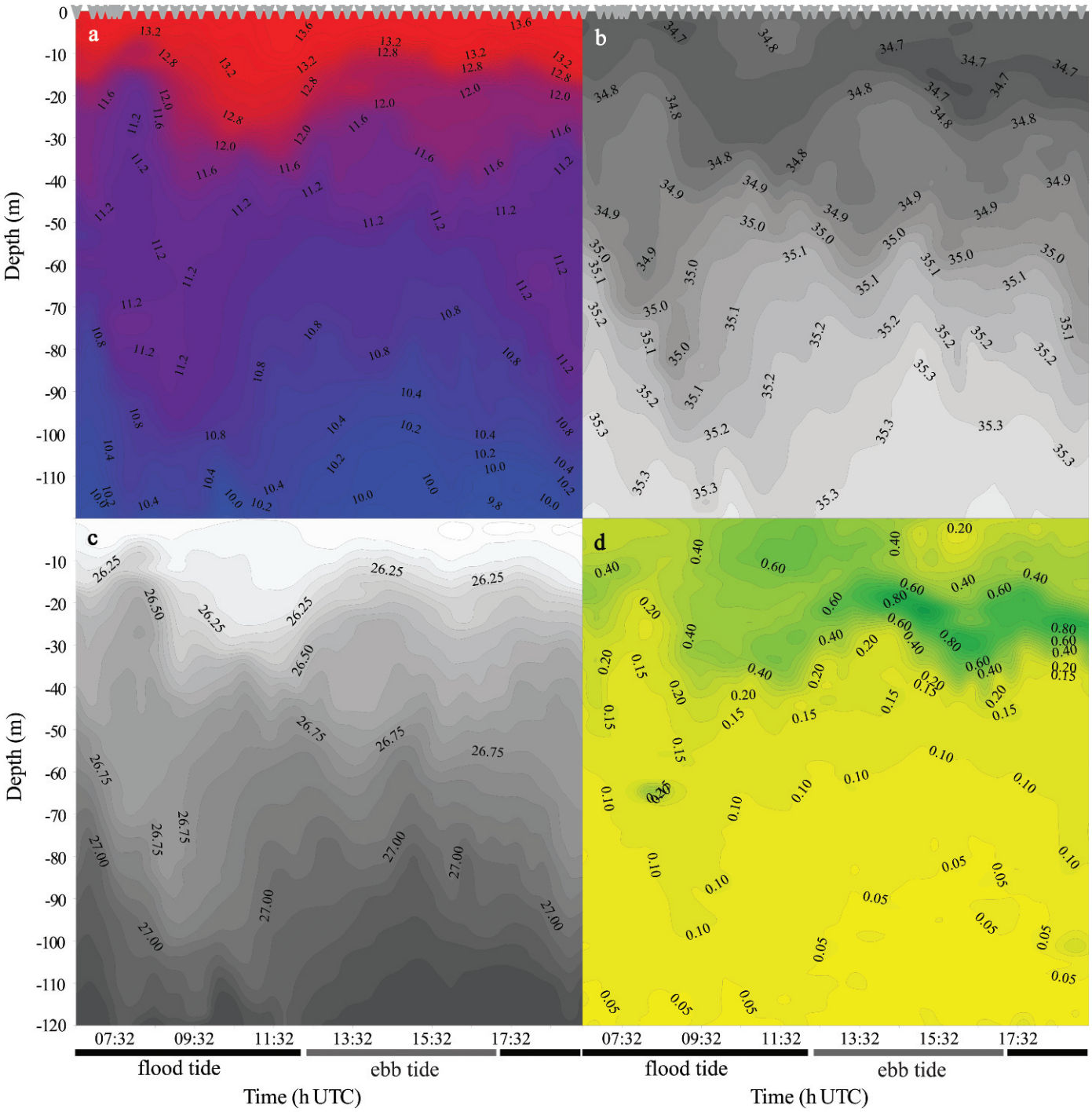

Fig. 5. CTD yo-yo series made on 20 June 2007 on top of Mingulay Reef 1 near Sta. 55 (gray arrows are individual CTD locations). Profiles show: (a) temperature (°C), (b) salinity (‰), (c) density (sigma-theta, kg m^{-3}), and (d) fluorescence (Chl *a*, $\mu g\ L^{-1}$). Time of slack tide between flood and ebb on the reef top (~140 m depth) was 12:00 h UTC.

the profile, $\Delta\rho$ is the difference between surface and bottom density, and H is the water depth.

On the basis of this calculation, the conditions above Reef 1 result in a Froude number that is close to one (Fr = 1.08) near the peak tidal flow (u_{max} = 0.41 m s^{-1}, ρ = 1026.83 kg m^{-3}, $\Delta\rho$ = 1.18 kg m^{-3}, g = 9.81 m s^{-2}, H = 127 m). Therefore it is likely that hydraulic control forms as a depression in the density structure downstream of the reef, driving surficial waters downward. On the turn of the tide, as the flow weakens and reverses, the downstream depression propagates over the summit of the reef, washing the reef with surficial water. This sequence occurs on both phases of the tide, as observed in the pulses of warmer water in Fig. 3 on the ebb to flood tide, but is strongest on the flood to ebb because of the asymmetric profile of the reef and strength of the tidal current.

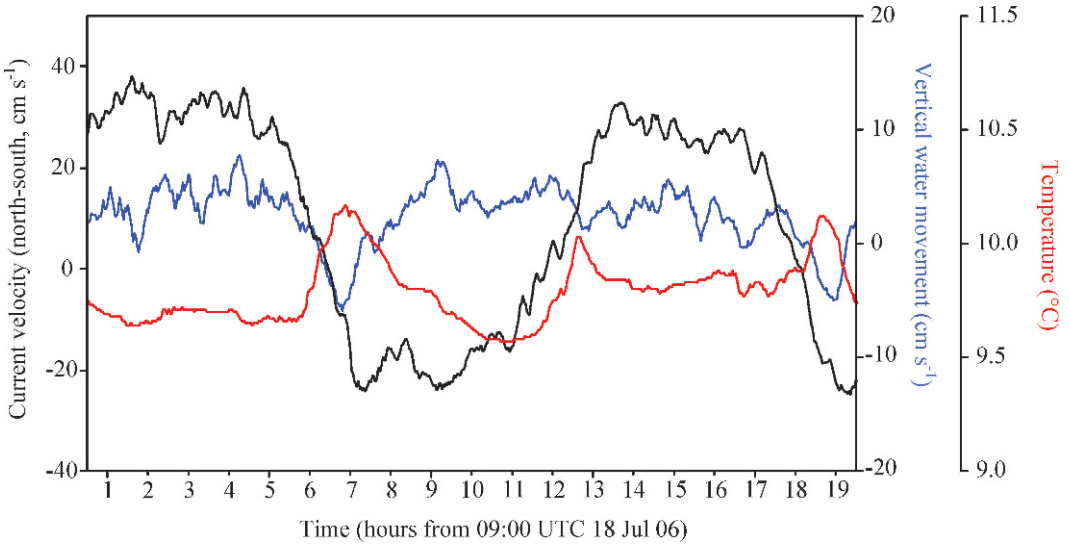

Fig. 6. Vertical water movement (blue line), N-S current speed component (black line), and water temperature (red line) recorded by a moored 3D current meter (Sta. 89) between 09:00 h UTC 18 July 2006 and 04:00 h UTC the following morning. The negative vertical water movement at the onset of the ebb tide indicates a downward flow associated with the internal hydraulic jump.

Relationships between internal hydrodynamics impinging on topography and the abundance of suspension and filter-feeders at specific depths have been earlier suggested by Rice et al. (1990) and Frederiksen et al. (1992). The zonation of corals along the Faeroes plateau has been attributed to increased surface production resulting from intensified vertical mixing. The mixing is generated by internal waves reflecting on a critical slope. Larger particles produced in the mixing zone would sink down rather than be moved away by the currents (Frederiksen et al. 1992). The sponge belt along the slope of the Porcupine Seabight seems to relate to resuspension and mobilization of organic material from the seafloor by breaking internal waves (Rice et al. 1990). The pulse of surface productivity to the

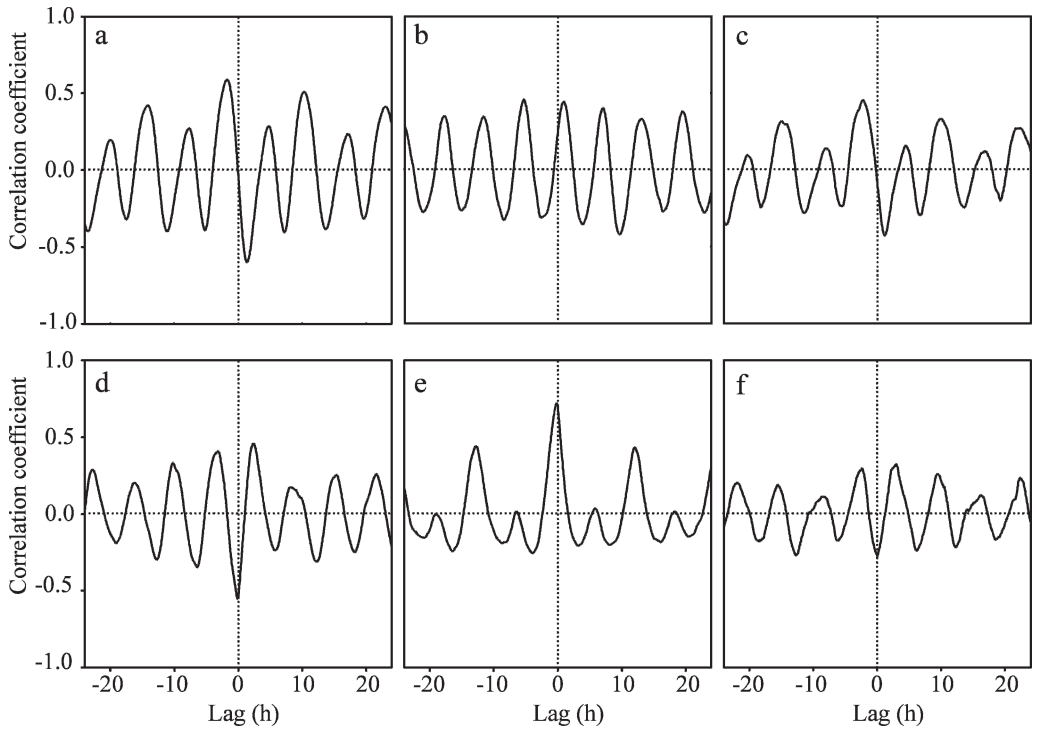

Fig. 7. Time-lagged relationships between recorded variables using cross-correlation from a current meter at Sta. 55 (with lags of ±24 h) between (a) current speed and temperature, (b) current speed and turbidity, (c) current speed and fluorescence, (d) temperature and turbidity, (e) temperature and fluorescence, (f) turbidity and fluorescence. Correlations range between −1 (negatively correlated) and 1 (positively correlated). Positive lags represent the primary axis offset against the secondary axis, whereas negative lags represent the secondary axis offset against the primary axis.

Mingulay reef is entirely driven by the internal motions due to hydraulic jump, as is clear from the strong correlations in Fig. 7.

As well as increasing the delivery of fluorescent particles, the rapid downwelling also displaces the colder water that is predominant throughout the reef area with warmer water (maximum recorded to date 10.25°C, an increase of approximately 0.75°C). Interestingly, a recent ecophysiological study found that the respiratory activity of *L. pertusa* increased by 50% in treatments that had a water temperature of 2°C higher than samples maintained at 9°C (Dodds et al. 2007). This adaptability of the metabolism of *L. pertusa*, combined with the increase in fresh organic matter and a slackening of current speed inducing polyp extension and feeding (A. J. Davies unpubl.), could allow the coral to take advantage of the transient change in conditions during the internal wave and the rapid downwelling event. However, it is not yet clear whether this relationship is actually beneficial for *L. pertusa*. Dodds et al. (2007) suggest that such temperature increases and the resultant effects on the metabolism of *L. pertusa* could lead to starvation if not met with sufficient food input (Newell and Branch 1980). Further research is required to fully understand the link between the rapid downwelling and the response of *L. pertusa*.

Besides the fresh particles delivered by the rapid downwelling of water after slack tide, corals on the Mingulay Reef also receive particles that are advected during peak flood and ebb currents when the surficial water on the reef is replaced by colder and more turbid water. This is illustrated by the significant positive correlation between current speed and turbidity in Fig. 7b. The time lag of 1 h between peak currents and high turbidity suggests that local resuspension on the reef top is less important than horizontal advection of particles with the tidal current. The importance of advection as a turbidity source on the reef is supported by the cross-reef profile generated from CTD transects in 2006. This process is equivalent to the widespread concept that current acceleration on topography promotes advection of food for cold-water corals (Thiem et al. 2006). The high maximum current speeds may also aid in keeping the living reef structure relatively clear of deposited sediment (White et al. 2005).

One example is given in Fig. 4d; this profile shows turbid water upwelling on the reef face. The higher turbidity in the advected water is most likely due to the fine silty sediment surrounding the reef area that becomes entrained in the bottom water because of frictional turbulence. As current speeds on top of the reef are three to four times higher compared with its sloping base, delivery of particles accounting for the turbidity is likewise enhanced. The turbid water is related to low fluorescence (Figs. 4c,d, 7f). The salinity profile suggests that it originates from deep water outside of the Minch (Fig. 4b; Savidge and Lennon 1987). However, the quantity of chlorophyll *a* appears to be an order of magnitude lower compared with earlier observations (Savidge and Lennon 1987). The lower fluorescence may indicate that this water has a long residence time in the benthic boundary layer before it reaches the reef (Ritzrau et al. 1997).

In conclusion, the *L. pertusa* reef communities at Mingulay Reef 1 are potentially fueled by two distinct mechanisms. First, a hydraulic jump and internal wave causes tidal-period rapid downwelling, which drives fresh organic matter from surface water layers toward the reef. This mechanism appears consistent and predictable over longer periods, as shown by observations in two successive years and a 3-month-long mooring deployment (Fig. 3b). Second, accelerated tidal currents on the reef top enhance the delivery of particles suspended in deeper water that is being advected toward the reef. The particle quality of the latter may be low, as indicated by reduced fluorescence levels. Assessment of particle quality is a vital next step toward understanding food supply to the Mingulay Reef complex. A further step is to collect information on the short-term in situ feeding behavior of cold-water corals, such as polyp extension cues, current shear tolerances, and food preferences.

References

Dodds, L. A., J. M. Roberts, A. C. Taylor, and F. Marubini. 2007. The cold-water coral *Lophelia pertusa* (Scleractinia) reveals metabolic tolerance to temperature and dissolved oxygen change. J. Exp. Mar. Biol. Ecol. **349:** 205–214.

Duineveld, G. C. A., M. S. S. Lavaleye, and E. M. Berghuis. 2004. Particle flux and food supply to a seamount cold-water coral community (Galicia Bank, NW Spain). Mar. Ecol. Prog. Ser. **277:** 13–23.

———, ———, M. J. N. Bergman, H. C. de Stigter, and F. Mienis. 2007. Trophic structure of a cold-water coral mound community (Rockall Bank, NE Atlantic) in relation to the near-bottom particle supply and current regime. Bull. Mar. Sci. **81:** 449–467.

Farmer, D., and L. Armi. 1999. The generation and trapping of solitary waves over topography. Science **283:** 188–190.

Flach, E., and L. Thomsen. 1998. Do physical and chemical factors structure the macrobenthic community at a continental slope in the NE Atlantic? Hydrobiologia **376:** 265–285.

Frederiksen, R., A. Jensen, and H. Westerberg. 1992. The distribution of the scleractinian coral *Lophelia pertusa* around the Faeroe Islands and the relation to internal tidal mixing. Sarsia **77:** 157–171.

Freiwald, A., V. Huhnerbäch, B. Lindberg, J. B. Wilson, and J. Campbell. 2002. The Sula Reef Complex, Norwegian shelf. Facies **47:** 179–200.

Gage, J. D., P. A. Lamont, K. Kroeger, G. L. J. Paterson, and J. L. G. Vecino. 2000. Patterns in deep-sea macrobenthos at the continental margin: Standing crop, diversity and faunal change on the continental slope off Scotland. Hydrobiologia **440:** 261–271.

Genin, A., P. K. Dayton, P. F. Lonsdale, and F. N. Speiss. 1986. Corals on seamount peaks provide evidence of current acceleration over deep-sea topography. Nature **322:** 59–61.

Henry, L.-A., and J. M. Roberts. 2007. Biodiversity and ecological composition of macrobenthos on cold-water coral mounds and adjacent off-mound habitat in the bathyal Porcupine Seabight, NE Atlantic. Deep-Sea Res. I **54:** 654–672.

Hovland, M. T., and E. Thomsen. 1997. Cold-water corals—are they hydrocarbon seep related? Mar. Geol. **137:** 159–164.

Hughes, D. J., and J. D. Gage. 2004. Benthic metazoan biomass, community structure and bioturbation at three contrasting deep-water sites on the northwest European continental margin. Prog. Oceanogr. **63:** 29–55.

Jonsson, L. G., P. G. Nilsson, F. Floruta, and T. Lundälv. 2004. Distributional patterns of macro- and megafauna associated with a reef of the cold-water coral *Lophelia pertusa* on the Swedish west coast. Mar. Ecol. Prog. Ser. **284:** 163–171.

Kano, A., and others. 2007. Age constraints on the origin and growth history of a deep-water coral mound in the northeast Atlantic drilled during Integrated Ocean Drilling Program Expedition 307. Geology **35:** 1051–1054.

Kiriakoulakis, K., E. Fisher, G. A. Wolff, A. Freiwald, A. Grehan, and J. M. Roberts. 2005. Lipids and nitrogen isotopes of two deep-water corals from the North-East Atlantic: Initial results and implications for their nutrition, p. 715–729. *In* A. Freiwald and J. M. Roberts [eds.], Cold-water corals and ecosystems. Springer-Verlag.

———, A. Freiwald, E. Fisher, and G. A. Wolff. 2007. Organic matter quality and supply to deep-water coral/mound systems of the NW European Continental Margin. Int. J. Earth Sci. **96:** 159–170.

Linnaeus, C. 1758. Systema Naturae per regna tria naturae, secundum classes, ordines, genera, species, cum chararteibus, differentiis, synonymis, locis (Holmiae: Laurentii Salvii), Stockholm.

Mienis, F., H. C. de Stigter, M. White, G. C. A. Duineveld, H. de Haas, and T. C. E. van Weering. 2007. Hydrodynamic controls on cold-water coral growth and carbonate-mound development at the SW and SE Rockall Trough margin, NE Atlantic Ocean. Deep-Sea Res. I **54:** 1655–1674.

Mortensen, P. B., M. T. Hovland, J. H. Fosså, and D. M. Furevik. 2001. Distribution, abundance and size of *Lophelia pertusa* coral reefs in mid-Norway in relation to seabed characteristics. J. Mar. Biol. Assoc. UK **81:** 581–597.

Nash, J. D., and J. N. Moum. 2001. Internal hydraulic flows on the continental shelf: High drag states over a small bank. J. Geophys. Res. **106:** 4593–4612.

Newell, R. C., and G. M. Branch. 1980. The influence of temperature on the maintenance of metabolic energy balance in marine invertebrates. Adv. Mar. Biol. **17:** 329–396.

Rice, A., M. Thurston, and A. New. 1990. Dense aggregations of a hexactinellid sponge, *Pheronema carpenteri*, in the Porcupine Seabight (northeast Atlantic Ocean), and possible causes. Prog. Oceanogr. **24:** 179–96.

Ritzrau, W., L. Thomsen, R. J. Lara, and G. Graf. 1997. Enhanced microbial utilisation of dissolved amino acids indicates rapid modification of organic matter in the benthic boundary layer. Mar. Ecol. Prog. Ser. **156:** 43–50.

Roberts, J. M., C. J. Brown, D. Long, and C. R. Bates. 2005. Acoustic mapping using a multibeam echosounder reveals cold-water coral reefs and surrounding habitats. Coral Reefs **24:** 654–669.

———, L.-A. Henry, D. Long, and J. P. Hartley. 2008. Cold-water coral reef frameworks, megafaunal communities and evidence for coral carbonate mounds on the Hatton Bank, north east Atlantic. Facies **54:** 297–316.

———, A. J. Wheeler, and A. Freiwald. 2006. Reefs of the deep: The biology and geology of cold-water coral ecosystems. Science **213:** 543–547.

Rogers, A. D. 1999. The biology of *Lophelia pertusa* (Linnaeus 1758) and other deep-water reef-forming corals and impacts from human activities. Int. Rev. Hydrobiol. **84:** 315–406.

Savidge, G., and H. Lennon. 1987. Hydrography and phytoplankton distributions in north-west Scottish waters. Cont. Shelf Res. **7:** 45–66.

Thiem, Ø., E. Ravagnan, J. H. Fosså, and J. Berntsen. 2006. Food supply mechanisms for cold-water corals along a continental shelf edge. J. Mar. Syst. **26:** 1481–1495.

Valle-Levinson, A., and R. E. Wilson. 1994. Effects of sill bathymetry, oscillating barotropic forcing and vertical mixing on estuary ocean exchange. J. Geophys. Res. Oceans **99:** 5149–5169.

van Weering, T. C. E., H. de Haas, H. C. de Stigter, H. Lykke-Andersen, and I. Kouvaev. 2003. Structure and development of giant carbonate mounds at the SW and SE Rockall Trough margins, NE Atlantic Ocean. Mar. Geol. **198:** 67–81.

White, M., I. Bashmachnikov, J. Aristegui, and A. Martins. 2007. Physical processes and seamount productivity, p. 65–84. *In* T. Pitcher, T. Morato, P. Hart, M. Clark, N. Haggan, and R. Santos [eds.], Seamounts: Ecology, fisheries & conservation. Blackwell.

———, C. Mohn, H. C. de Stigter, and G. Mottram. 2005. Deep-water coral development as a function of hydrodynamics and surface productivity around the submarine banks of the Rockall Trough, NE Atlantic, p. 503–514. *In* A. Freiwald and J. M. Roberts [eds.], Cold-water corals and ecosystems. Springer-Verlag.

Williams, T., and others. 2006. Cold-water coral mounds revealed. EOS **87:** 526–527.

Edited by: Anthony Larkum

Received: 15 June 2008
Accepted: 9 October 2008
Amended: 9 October 2008